Proceedings of

12th Structural Engineering Convention-An International Event (SEC 2022)

Available at https://asps-journals.com/index.php/acp

Nonlocal modeling of crack-interface interaction in a composite system

Dhaladhuli Pranavi[1,*], Amirtham Rajagopal [1]

[1] Department of civil engineering, Indian Institute of Technology Hyderabad, India

Paper ID - 010533

Abstract

The mechanical response and the fracture phenomena in a composite system not only depend on the elastic and fracture properties of individual constituents but also on additional parameters such as fiber alignment, fiber volume fraction, interface properties and laminate layup. Fiber alignment is one such parameter that governs the design of the composite according to the purpose required. In the present work, a nonlocal approach combined with a cohesive zone model is proposed and implemented in finite element framework. The proposed model can capture different failure phenomena in a matrix- fiber system. The influence of various properties of fiber, matrix, and the fiber-matrix interface on the mechanical response of the composite system is studied. An exponential coupled cohesive zone law is considered for modeling fiber-matrix interface. Smeared representation of crack and interface are considered in the analysis. The results are validated with numerical simulations present in the literature.

Keywords: Nonlocal, Fiber-matrix interface, Heterogeneous, Cohesive zone law, Fracture

1. Introduction

Unlike homogeneous materials, composites offer superior qualities such as enhanced stiffness and strength for lightweight materials. Understanding fracture in anisotropic material such as composite is much more complex when compared to the brittle/ductile fracture in isotropic materials such as steel and aluminum. To predict the failure, the independent failure mechanisms like fiber/matrix failure, fiber-matric debonding, and delamination between the laminae needs to be examined [1], [2]. The fiber- matrix interface and the interface between the laminae play a pivotal role in determining the overall strength and toughness of the composite system. Therefore, accurate modeling of damage/fracture at the interface is required.

Finite element analysis has been adopted to understand the failure phenomena in composites [3]. Cohesive zone model is adopted to model various modes of failure in laminated composites in [4]. Numerical methods such as continuum damage models [5], XFEM [6], peridynamics [7], gradient damage models [8] can model composite fracture/failure. To model fracture and/or damage, a new approach GraFEA which is a graph-based finite element approach is proposed and implemented in [9]. Smeared crack models like phase field method (PFM) have become popular to model complex behavior. In PFM, variational principles are used to minimize the global energy functional [10].The effect of fracture properties in nanocomposites is studied using PFM in [11]. Various failure modes at meso structural level in a composite are analyzed in [12].

Anisotropic surface energy [13] is introduced based on structural tensors [14] in the total energy of the system to model the crack propagation using phase field approach. Definite phase-fields related to individual damage mechanism have been proposed in [15] and [16]. In [17], gradient-enhanced damage model is adopted to model intralaminar and translaminar brittle fracture. PFM+Anisotropy model is adopted to study delamination under different modes undergoing finite strain in [2]. The interaction of interface with crack is modeled using combined phase field approach and cohesive zone model in isotropic materials [18] and anisotropic composites [19].

The main focus of the present work is to understand the effect of fiber orientation of a fiber reinforced composite system. The crack propagation in a laminated fiber reinforced composite stacked with spatially varying unidirectional and woven fibers is studied for different configurations. The interaction between the anisotropic crack and the interface is studied by varying the relative stiffness of the interface to that of the bulk.

2. Methodology

Consider solid heterogeneous body Ω consists of two different fiber reinforced composites Ω_1 and Ω_2 such that $\Omega_1 \cup \Omega_2 = \Omega$ as shown in Figure 1. Let Γ and Γ_I represent the crack and the interface between the two composites respectively.

*Corresponding author. Tel: +918813971517; E-mail address: ce18m20p000001@iith.ac.in

Proceedings of the 12th Structural Engineering Convention (SEC 2022), NCDMM, MNIT Jaipur, India| 19-22 December, 2022

Published online: December 19, 2022

doi:10.38208/acp.v1.483

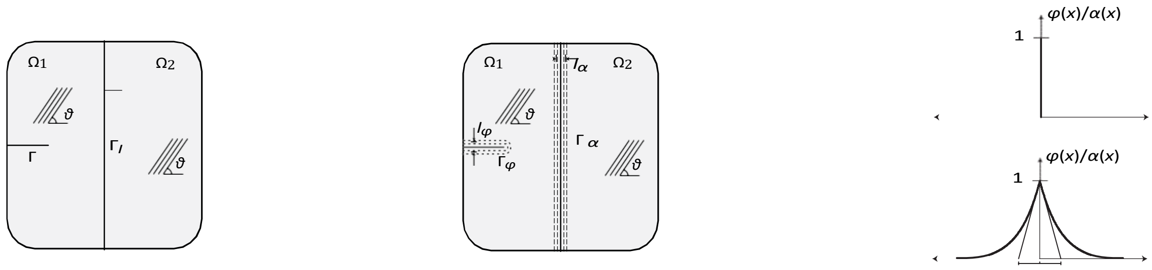

(a) (b) ©

Figure 1: Schematic representation of (a) sharp crack Γ and sharp interface Γ_I, (b) regularized crack Γ and regularized interface Γ_α, and (c)sharp and diffusive crack/interface topology.

$$E = \Psi_e(\varepsilon^e;\varphi)d\Omega + G_c d\Gamma + \Psi_I([uj])\, d\Gamma_I \quad (1)$$

$$E = \Psi_e(\varepsilon^e;\varphi)\, d\Omega + G_c\gamma_\varphi(\varphi, \nabla\varphi, A)\, d\Omega + \Psi_I(j)\, \gamma_\alpha(\alpha, \nabla\alpha)\, d\Omega \quad (2)$$

where $\varphi(x)$ represent the crack phase field variable, $\alpha(x)$ represent the interface phase field variable and are expressed as $\varphi(x) = e^{-|x|/l}\varphi$and $\alpha(x) = e^{-|x|/l}\alpha$ respectively. The diffused width of crack and interface are denoted by $l_\varphi$and l_α, $G_c$is the fracture toughness, $j(x)$ is the jump in the displacements across the diffused interface, $\gamma_\varphi(\varphi)$, $\gamma_\alpha(\alpha)$ represent the crack density and interface density functions per unit volume.

Energy functions

The energy density function Ψ_e in Eq. (2) is defined as

$$\Psi e\ (\varepsilon^e;\varphi) = g(\varphi)\Psi o\ (\varepsilon^e, a) \quad (3)$$

$g(\varphi)$ represents the degradation function. In the present work, a quadratic form $g(\varphi) = (1 - \varphi)^2$ is adopted for the analysis.

$$\Psi o\ (\varepsilon^e, a) = \Psi iso\ (\varepsilon^e) + \Psi ani\ (\varepsilon^e, a) \quad (4)$$

Ψ^{iso} represents the matrix contribution and Ψ^{ani} represents the fiber contribution.

$$\Psi iso\ (\varepsilon^e) = (\lambda/2).(tr\varepsilon^e)^2 + \mu\ (\varepsilon^e : \varepsilon^e) \quad (5)$$

$$\Psi^{ani}(\varepsilon^e, a) = \mu(\varepsilon^e : a)^2 \quad (6)$$

λ and μ are the lam´e's constants and $\mu_f$is a stress like material parameter related to fibers. The regularized crack functional for an anisotropic material can be written as

$$\gamma(\varphi, \nabla\varphi, A) = (1/2l_\varphi)\varphi^2 + l^2\, \nabla\varphi \cdot A\, \nabla\varphi$$
$$A = I + \beta a,\ a = f \otimes f,\ f = [\cos\theta, \sin\theta, 0]^T \quad (7)$$

A represents the anisotropic structural tensor, I is the second order identity tensor, f is the unit vector corresponding to the fiber orientation θ with respect to the global X axis and β denotes the anisotropy parameter.

Cohesive zone model

The constitutive relation at the interface is given by a cohesive zone law which relates the interface traction with its corresponding separation [20], [21]. The interface is characterized by the existence of a potential function $\Psi_I$which describes the coupled traction-separation. For the present work, exponential coupled traction separation law is adopted, see Figure 2[22].

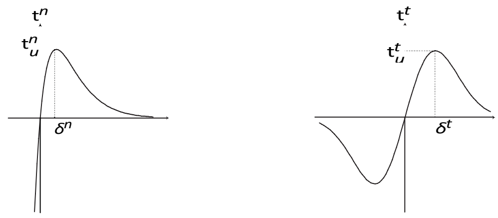

(a) (b)

Figure 2: Exponential cohesive zone law depicting (a)Normal traction separation and (b)Tangential traction separation.

The potential function is given as:

$$\Psi_I\left(j^n, j^t\right) = \Psi_n^I\left[1 - \left(1 + \frac{j^n}{\delta^n}\right)\exp\left(-\frac{j^n}{\delta^n}\right)\exp\left(-\left(\frac{j^t}{\delta^t}\right)^2\right)\right] \quad (8)$$

The traction vector can be obtained as:

$$\mathbf{t} = \frac{\partial \Psi_I}{\partial \mathbf{j}}, \quad \mathbf{j} = [j^n, j^t]^T \quad (9)$$

Governing Equations

Variation of Eq. (2) with respect to displacement u and phase field φ results in the following equations

$$\int_\Omega \frac{\partial \Psi_e}{\partial \varepsilon^e} : \varepsilon^e(\delta\mathbf{u})\ \ d\Omega + \int_\Omega \frac{\partial \Psi_I}{\partial \boldsymbol{j}}\ \delta\mathbf{j}\ \gamma(\alpha, \nabla\alpha)\ \ d\Omega = 0 \quad (10)$$

$$\int_\Omega g'(\phi)\Psi_o\ d\Omega + \int_\Omega \mathcal{G}_c\delta\gamma(\phi, \nabla\phi, \boldsymbol{A})\ d\Omega = 0 \quad (11)$$

The interface energy density function can be written as

$$\gamma(\alpha, \nabla\alpha) = \frac{1}{2l_\alpha}\left(\alpha^2 + l_\alpha^2 \nabla\alpha \cdot \nabla\alpha\right) \quad (12)$$

The crack driving force H can be obtained from the ratio Ψ_o/G_c, which is defined for each individual damage mode corresponding to matrix(isotropic) and fiber(anisotropic) as:

$$\mathcal{H} = \frac{\Psi_o^{iso}}{\mathcal{G}_c^{iso}} + \frac{\Psi_o^{ani}}{\mathcal{G}_c^{ani}} \quad (13)$$

G^{iso} and G^{ani} denote the critical energy release rate corresponding to matrix and fiber respectively.

3. Numerical simulation

The proposed formulation is demonstrated through two examples, (a) Open hole tension test and (b) crack-interface interaction in a composite laminate. Four noded quadrilateral elements are used for the analysis. Plane strain conditions are assumed.

3.1. Open hole tension test

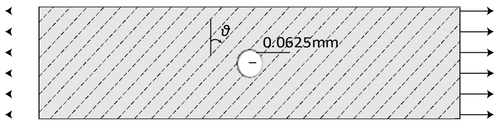

Figure 3: Geometry and boundary conditions of the OHT specimen.

Inthisexample,arectangularspecimenwithacentralcircularhole isconsideredasshowninFigure3.The material properties are taken as: Longitudinal Young's modulus E_1 = 26.5 GPa, Transverse Young'smodulus E_2=2.6GPa,Shear modulus G_{12}=1.3GPa,Poisson'sratiov_{12}=0.35,the criticalenergyreleaserateofmatrixandfiber aregivenasG^{iso}= 0.622N/mm,G^{ani}= 106.3N/mm.l_φ=l_α=0.012mm.Theobjectivesofthisexamplear etounderstandtheinfluenceof(a)fiberorientation$\theta$and(b)anis otropyparameterβonthemechanicalresponseandthecrackpro pagation of the unidirectional fiberreinforced composite system.For the firststudy, fibers of three different orientations namely, (i)θ = 15°, (ii)θ = 30°and (iii)θ = 45° are considered for a fixed value of anisotropy parameter β = 25.For the second study, fiber orientation is fixed to be θ = 45° and the anisotropy parameter is varied as (i)β = 0, (ii)β = 25 and (iii)β = 50.

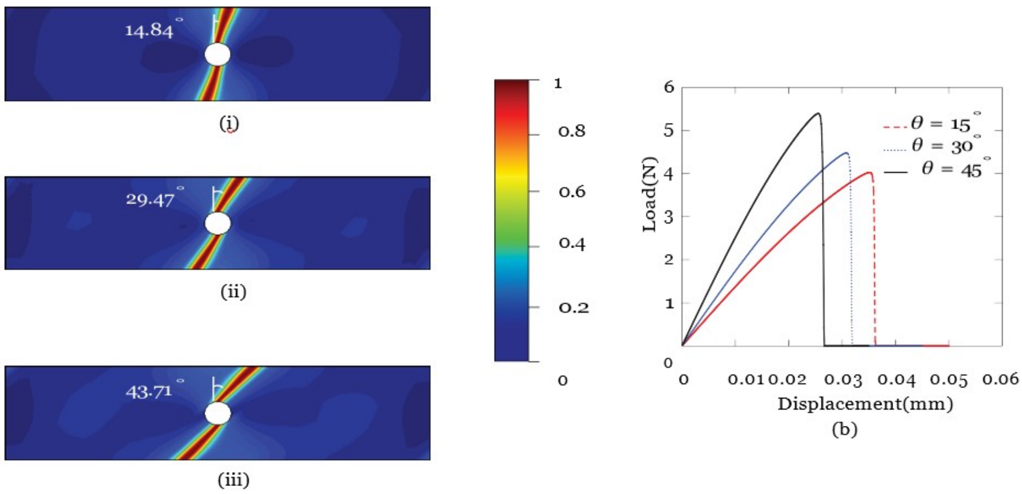

(a)

Figure 4: (a)Evolution of anisotropic crack phase field for (i)θ = 15◦, (ii)θ = 30◦, (iii)θ = 45◦ and (b)Load displacement curves for fiber orientations θ = 15◦, θ = 30◦, θ = 45◦ for β = 25.

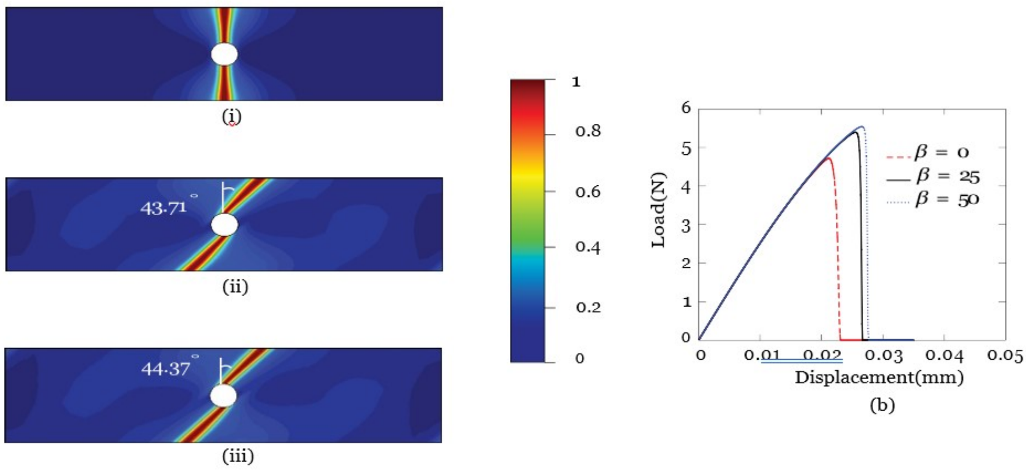

(a)

Figure 5: (a)Evolution of anisotropic crack phase field for (i)β = 0, (ii)β = 25, (iii)β = 50 and (b)Load displacement curves for fiber orientations β = 0, β = 25, β = 50 for θ = 45◦.

The crack propagation and load displacement curves for the two studies are plotted in Figure 4 and Figure 5 respectively. The crack propagation in Figure 4 is along the fiber orientation for all the angles and the failure load increases with increase in fiber orientation. From Figure 5, it is observed that for $\beta = 0$, which is an isotropic case, the crack is perpendiclar to the loading direction. As β value increases, the crack angle is more towards the fiber orientation. With increase in β value, the failure load increases.

3.2. Crack-interface interaction in a laminate

A spatially varied composite laminate made up of different fibreorientations and is considered to understand the interaction of crack with interface under Mode I loading. The geometry and boundary conditions are depicted in Figure 6. The interface can be distinguished as stiff or soft interface based on the relative values of critical energy release rate of the interface to that of the bulk. If the interface stiffness is high, it is stiff interface and viceversa. The material properties are taken as follows:

Material I: $(E_1)_I = 171$ GPa, $(E_2)_I = 9.08$ GPa, $(G_{12})_I = 5.29$ GPa, $\nu_{12} = 0.32$, $(\mathcal{G}_c^{\text{ani}})_I = 97.8\text{N/mm}$, $(\mathcal{G}_c^{\text{iso}})_I = 0.788\text{N/mm}$, $l_\phi = l_\alpha = 0.012\text{mm}$,

Material II: $(E_1)_{II} = \text{m} \times (E_1)_I$, $(E_2)_{II} = \text{m} \times (E_2)_I$, $(G_{12})_{II} = \text{m} \times (G_{12})_I$, $\nu_{12} = 0.32$, $(\mathcal{G}_c^{\text{ani}})_{II} = (\mathcal{G}_c^{\text{ani}})_I/\text{mN/mm}$, $(\mathcal{G}_c^{\text{iso}})_{II} = (\mathcal{G}_c^{\text{iso}})_I/\text{mN/mm}$

Interface: $\text{t}_u^n = \text{t}_u^t = 1$ MPa. For stiff-interface $\mathcal{G}_c^I = \mathcal{G}_c^{\text{ani}}$, for soft interface, $\mathcal{G}_c^I = 0.00025 \times \mathcal{G}_c^{\text{ani}}$.

The analysis is done for two values of m which are (i)m= 0.8 and (ii)m= 1.2.

The crack propagation for two cases for stiff and soft interfaces are plotted in Figure 7. It is observed that the crack propagation is similar for both the values of m for stiff and soft interfaces. For a stiff interface model, the crack follows the fiber orientation in all the composite layup without deflecting along the interface and for a soft interface model, the crack after reaching the interface, deflects along the interface and then penetrates into the next composite layup. From the load displacement curves plotted in Figure 8, it is observed that the failure load is high for stiff interface and also for higher values of m.

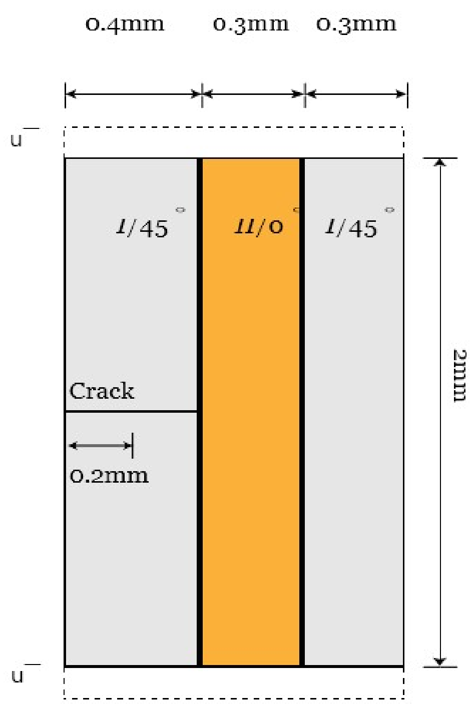

Figure 6: Geometry and boundary conditions

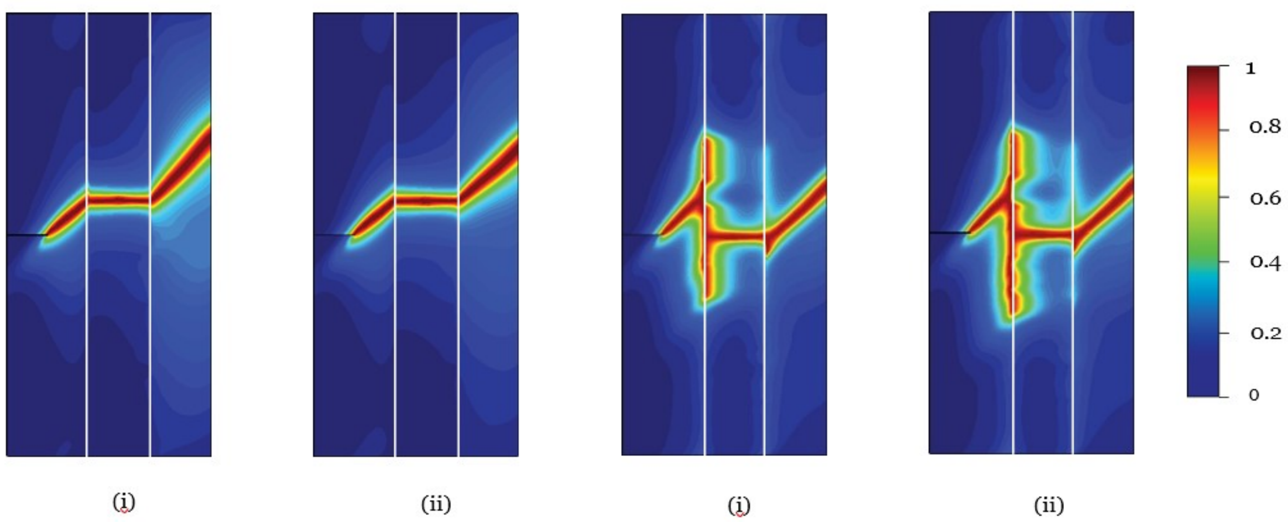

Figure 7: Evolution of anisotropic crack phase field for (a)Stiff interface (i) m=0.8, (ii) m=1.25 and (b)Soft interface (iii) m=0.8, (iv) m=1.25.

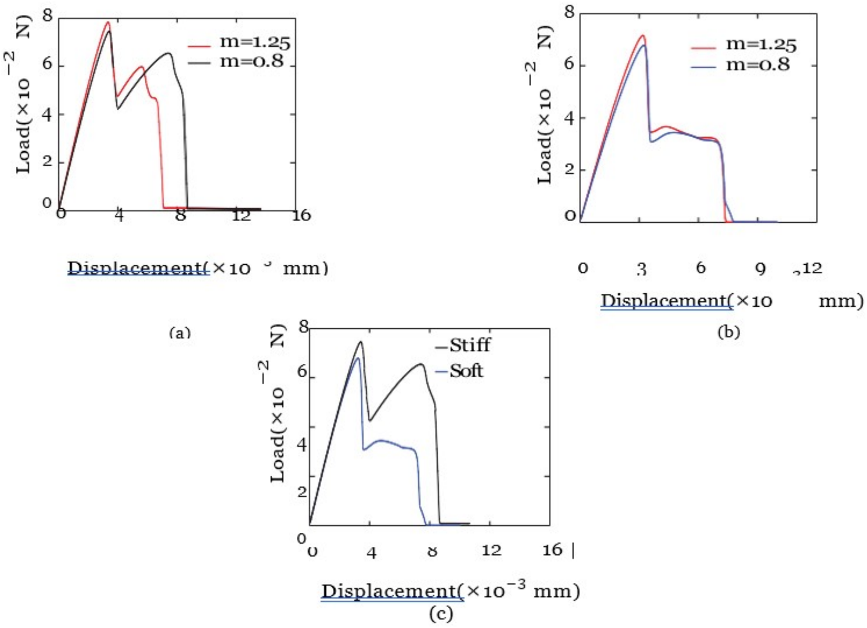

Figure 8: Load-displacement curves for (a)Stiff interface m=0.8, m=1.25, (b)Soft interface m=0.8, m=1.25, (c)Stiff interface and Soft interface for m=0.8.

1. Conclusion

For a composite reinforced with unidirectional fibers, as the fiber orientation increases, the failure load of the specimen increases. The predicted crack path predicted by the proposed model is along the fiber orientation for β = 25, 50. β = 0 depicts the isotropic case, therefore the crack path is perpendicular to the loading direction. As the value of anisotropy parameter β increases, the failure load increases and converges. When the crack interacts with the interface between two composites, the crack either deflects along the interface or penetrates through the interface based on the relative fracture toughness of the interface to that of the bulk.

Disclosures

Free Access to this article is sponsored by SARL ALPHA CRISTO INDUSTRIAL.

References

[1] P. Camanho and S. Hallett. Numerical modelling of failure in advanced composite materials. Elsevier, USA, 2015.

[2] F. A. Denli, O. O Gu¨ltekin, G. A. Holzapfel, and H. Dal. A phase-field model for fracture of unidirectional fiber-reinforced polymer matrix composites. Comput. Mech., 65:1149–1166, 2020.

[3] R. S. Barsoum. On the use of isoparametric finite elements in linear fracture mechanics. Int. J. Numer. Methods Eng., 10:25–37, 1976.

[4] L. Zhao, Y. Gong, J. Zhang, Y. Chen, and B. Fei. Simulation of delamination growth in multidirectional laminates under mode i and mixed mode i/ii loadings using cohesive elements. Compos. Struct., 116:509–522, 2016.

[5] J. Reinoso, G. Catalanotti, A. Bla´zquez, P. Areias, P. P. Camanho, and F. Par´ıs. A consistent anisotropic damage model for laminated fiber-reinforced composites using the 3d-version of the puck failure criterion. Int. J Solids Struct., 126-127:37–53, 2017.

[6] S. Yazdani, W. J. H. Rust, and P. Wriggers. An xfem approach for modelling delamination in composite laminates. Compos. Struct., 135:353–364, 2016.

[7] S. Yazdani, W. J. H. Rust, and P. Wriggers. Dual-horizon peridynamics: A stable solution to varying horizons. Comput. Methods Appl. Mech. Eng., 318:762–782, 2017.

[8] Z. P. Bazant and G. Pijaudier-Cabot. Nonlocal continuum damage, localization instability and convergence. J. Appl. Mech., 55:287–293, 1988.

[9] P. Khodabakhshi, J. N. Reddy, and A. Srinivasa. Grafea: a graph-based finite element approach for the study of damage and fracture in brittle materials. Meccanica, 51:3129–3147, 2016.

[10] B. Bourdin, G. Francfort, and J. Marigo. Numerical experiments in revisited brittle fracture. J. Mech. Phys. Solids., 48:797–826, 2000.

[11] K. M. Hamdia, M. A. Msekh, M. Silani, N. Vu-Bac, X. Zhuang, T. Nguyen-Thoiab, and

T. Rabczuk. Uncertainty quantification of the fracture properties of polymeric nanocomposites based on phase field modeling. Compos. Struct., 133:1177–1190, 2015.

[12] J. J. Espadas-Escalante and P. Isaksson. Mesoscale analysis of the transverse cracking kinetics in woven composite laminates using a phase-field fracture theory. Eng. Fract. Mech., 216:106523, 2019.

[13] B. Li and C. Maurini. Crack kinking in a variational phase-field model of brittle fracture with strongly anisotropic surface energy. J. Mech. Phys. Solids., 125:502–522, 2019.

[14] T. T. Nguyen, J. Re´thore´, and M. C. Baietto. Phase field modelling of anisotropic crack propa- gation. Eur. J. Mech. A Solids., 65:279–288, 2017.

[15] J. Bleyer and R. Alessi. Phase-field modeling of anisotropic brittle fracture including several damage mechanisms. Comput. Methods Appl. Mech. Eng., 336:213–236, 2018.

[16] G. Y. Qiu and T. J. Pence. Remarks on the behavior of simple directionally reinforced incom- pressible nonlinearly elastic solids. J. Elast., 49:1–30, 1997.

[17] A. Quintanas-Corominas, J. Reinoso, E. Casoni, A. Turon, and J. A. Mayugo. A phase field approach to simulate intralaminar and translaminar fracture in long fiber composite materials. Compos. Struct., 220:899–911, 2019.

[18] P. Dhaladhuli, R. Amirtham, and J. N. Reddy. Interaction between interfacial damage and crack propagation in quasi-brittle materials. Mech. Adv. Mater. Struct., 2021.

[19] D. Pranavi, A. Rajagopal, and J. N. Reddy. Interaction of anisotropic crack phase field with interface cohesive zone model for fiber reinforced composites. Compos. Struct., 270:114038, 2021.

[20] D. S. Dugdale. Yielding of steel sheets containing slits. J. Mech. Phys. Solids, 8:100–104, 1960.

[21] G. I. Barenblatt. The formation of equilibrium cracks during brittle fracture. general ideas and hypotheses. axially-symmetric cracks. J. Appl. Math. Mech., 23:622–644, 1959.

[22] M. J. Van den Bosch, P. J. G. Schreurs, and M. G. D. Geers. An improved description of the exponential xu and needleman cohesive zone law for mixed-mode decohesion. Eng. Fract. Mech., 73:1220–1234, 2006.